Comparison of Obtained Geometric Accuracy of a DGPS and Drone Acquired Stereo image

Olaleye J.B., Suru W.P., Odeyemi F.G., Alabi A.O.

Abstract- This work deals with comparing the geometric accuracy of a DGPS and that of a drone acquired stereo image system from Trimble UX-5 Unmanned Aircraft System (UAS) using the methods of metrology. Measurement of image coordinates for control, check and detail points were done on the stereo image using AutoCAD and the ground coordinates of the points were obtained using Promark 3 Differential Global Positioning System (DGPS) equipment. The data obtained was used in a MATLAB program to compute for 3D object space coordinate of points. The control and check point's differences between two techniques are determined and the root mean square errors (RMSE) of the 3D coordinates are for control points ±0.392m , ±0.108m , ± 0.273m and it planimetric accuracy is 0.407m (40.7cm); for both control and check points in X, Y and Z is ±0.430m, ±0.152m,± 0.480m and it planimetric accuracy is 0.456m (45.6cm) and for only check points in X, Y and Z is ±0.337m, ±0.232m,±0.164m and it planimetric accuracy is 0.409m (40.9cm). The relative distances between the coordinates of points and areas from the two techniques are determined, their relative percentage errors and accuracies are deduce from this. Finally, analysis of variance (ANOVA) is used to ascertain whether the means of the relative distances and the z-coordinates between the techniques are the same. Results obtained shows that the □,y,□ coordinates computed from photogrammetry methods are accurate in terms of their linear, area accuracy and elevation but the latter show a weak result may be due to effects of lens aberration, wind, atmospheric refraction, banking, etc.

Index Terms-Conjugal ray, Coplanarity condition, DGPS, Drone, Monocomparator, Stereo image, UAV

1 INTRODUCTION

The Unmanned aerial systems (UAS), UAVs and drones are making the news almost every day, to the extent that some scholars are coining to the emergence of a new field term droneography. Unfortunately, these terms are often conflated and confused with large military drones which are changing the battleground from the field to some remote control station thousands of miles from where the war is being waged.[1] The UAS' used in this research have nothing to do with warfare and are a fraction of the size and weight. In fact, small UAVs have emerged from the design and manufacturing of (non-military) cell phones. Small, open source UAS' should therefore not be confused with military drones or even classified as a similar technology. However, this technology represents another technological leap much like GPS did in the late 1980s and early 1990s. By providing current, high resolution imagery it has the potential to create a model of the landscape that can be used to survey and map in a virtual mode thus drastically reducing the amount of fieldwork required and offering order of magnitude savings in time.[1]

The introduction of this technology does not suggest the end of fieldwork and surveying since the success of this surveying technique rests on the extent to which one can recognise and identify features (objects) on the landscape, or boundaries within the context of Geomatics and surveying.

Therefore, there are vast potential application of UAS' for mapping: Geomatics Engineering, defining cadastral boundaries, monitoring the construction of roads or buildings, urban planning, upgrading informal settlements, environmental monitoring, asset management, and several other activities that depend on geospatial data.

"Cunningham et al (as cited in [1] stated that several publications have dealt with the promise of UAS in the areas of property appraisal for taxation purposes", "Jazayeri et al (as cited in [1]) work on modeling buildings to develop a 3-D cadaster and various other areas that involve geospatial data". "Everaerts (as citied in [1]) lists numerous application areas including archeology, agriculture and monitoring of fires and traffic".

"Manyoky et al; Baiocchi; Neitzel and Klonowski (as cited in [1]) stated that this technology have been field tested but on a very limited area or on just one or two buildings". "Volkmann and Barnes [1], carried out tests to cover larger areas that would give us an idea of feasibility of using this technology for land adjudication or regularization. They collaborated with the private sector in Albania and involved local inhabitants and administrators as much as possible".

1.1 AIM

The aim of this paper is to compare Geometric accuracy obtained using DGPS and that of a drone acquired image system

1.2 OBJECTIVES

The objectives of this work are as follows:

i. To determine the coordinates of control and check points using differential Global positioning system.
ii. To obtain the geometric locations or positions of control and check points through acquired drone image.
iii. To compute the root mean squares errors of geometric points.
iv. To compute relative error and percentage relative error between different geometric points.
v. To compute relative error and percentage relative error of at least two area of triangle.
vi. To ascertain whether distances mean between GCPs obtained with DGPS and that obtained with drone stereo images are the same or insignificant
vii. To ascertain whether heights mean between GCPs obtained with DGPS and that obtained with drone stereo images are the same or insignificant

1.3 STUDY AREA

This project site is at Faculty of Education, university of Lagos, Akoka, Yaba, Lagos in the western part of Nigeria.

2.0 LITERATURES REVIEW

This work briefly describes the components of a UAS, focusing on vertical take-off and landing or VTOL vehicles and the descriptions of various capabilities of UAS were provided.

2.1 UAS COMPONENTS

According to [1], it consist of three fundamental components which all interact with each other at some point in the mapping process. These components are:

i. Unmanned aerial vehicle (UAV) carrying navigation equipment (advanced autopilot module - APM, GPS, inertial measurement unit - IMU), camera (off-the-shelf non-metric cameras are usually cheaper and lighter), battery (Lithium-polymer LiPo);
ii. Laptop or base station on which the initial flight planning is done and which shows real-time navigation, imagery and telemetry information (Lat, Long, GPS quality, etc.);
iii. Remote control (RC) transmitter which can be used to manually control the UAV and which receives basic data on the status of the vehicle (battery voltage, GPS quality, roll, pitch and heading).

2.2 CLASSES OF UAS

The UAS technology can be classified into two distinct categories – vertical takeoff and landing (VTOL or Rotary-winged) and fixed wing. VTOL vehicles are generally designed as multi-rotor copters with 3, 4 ('quadcopter'), 6 ('hexacopter') or 8 propellers ('octocopter') and Fixed wing UAVs are designed just like conventional aircraft that require forward motion to fly and space to take off and land while VTOL vehiclesrequire very little space for take-off, landing and have the capability to hover if so desired. VTOL UAVs are therefore preferable for smaller areas where high resolution imagery is required and fixed wing UAVs are likely more productive over large areas, although these will generally be at a lower resolution because of the speed at they must fly and the restrictions on camera shutter speeds and continuous exposure rates. When selecting a UAV it is important to consider whether coverage of a whole area is needed at the same time, or whether it is better to map incrementally as the spatial data is needed so that the data is more current. In this research, fixed wing was used to acquire images of Faculty of Education, university of Lagos, Akoka, Yaba, Lagos.

2.3 MAPPING

The documentation of the natural and cultural features of our world is a vivid task of many research areas and in the field of computational sciences, the reconstruction of cities has obtained a significant attention in recent years. Urban and rural reconstruction is an exciting area of research with several potential applications. Despite the high volume of previous work, there are many unsolved problems in developing countries, especially when it comes to the development of fully automatic algorithms.

Urban reconstruction is a wide spread domain. Practical fields that benefit from reconstructed three-dimensional urban models are multiple as well:

- In the entertainment industry, the storyline of several movies and computer games takes place in real cities. In order to make these cities believable at least some part of the models are obtained by urban reconstruction.
- Digital mapping for mobile devices, cars, and desktop computers requires two-dimensional and three dimensional urban models. Examples of such applications are Google Earth and Microsoft Bing Maps.
- Urban planning in a broad sense relies on urban reconstruction to obtain the current state of the urban environment. This forms the basis for developing future plans or to judge new plans in the context of the existing environment.

- Applications such as emergency management, civil protection, disaster control, and security training benefit from virtual urban worlds.

From the economic standpoint, there is an enormous benefit of being able to quickly generate high-quality digital worlds in the growing virtual consumption market to solve problems in the developing countries.

Urban habitats consist of many objects, such as people, cars, streets, parks, traffic signs, vegetation, and buildings. In this thesis, it focus on urban reconstruction, which is consider as the creation of 3D geometric models of urban areas, individual buildings, façades, and even their further details.

Most publications discussed in this survey were published in computer graphics, computer vision, and photogrammetry and remote sensing. There are multiple other fields that contain interesting publications relevant to urban reconstruction, e.g. machine learning, computer aided design, geo-sciences, mobile-technology, architecture, civil engineering, and electrical engineering. Our emphasis is the geometric reconstruction and we do not discuss aspects, like the construction of hardware and sensors, details of data acquisition processes, and particular applications of urban models.

There are various types of possible input data that is suitable as a source for urban reconstruction algorithms. Imagery is perhaps the most obvious input source. Common images acquired from the ground have the advantage of being very easy to obtain, to store, and to exchange.

Nowadays, estimated tens of billions of photos are taken worldwide each year, which results in hundreds of petabytes of data. Many are uploaded and exchanged over the Internet, and furthermore, many of them depict urban sites.

2.4 MAPPING METHODS

2.4.1 TOTAL STATION SURVEY

A Total Station combines a theodolite and an Electromagnetic Distance Meter (EDM) in one single instrument. This instrument requires two known survey stations for it usage. The theodolite is used to measure angles between the survey stations and points on objects while the EDM is used to measure slope distances from it to the object points. Angle and distance observations to the object can be used to accurately position relative to the survey station. Total Stations remain frequently used instruments for conducting topographic surveys in heritage recording projects “Ref. [2]”, “Ref. [3]”, “Ref. [4]”, “Ref. [5]” The user using this equipment measures only distinctive points that represent features, including edges and corners. “Ref. [6]”,“Ref. [2]” Individual point measurements are very accurate, but data collection is time consuming and this method has become less attractive for 3D reconstructionand thiscan be used to evaluate the accuracy of other recording techniques.

2.4.2 PHOTOGRAMMETRIC MAPPING

This technique uses spectral information (signal) reflected from an object to record and storeit within photographic images. “Clowes [7]; Girelli, Tini & Zanutta, [8]; Tack et al [9]; Yilmaz et al [10]) stated that digital technology has improved the use of photogrammetry in urban structures recording by speeding up data processing, providing cheaper equipment, and enable non-specialists to employ photogrammetric methods”. The technique is well suited for urban structures recording or mapping. “Ref. [8]”, “Ref. [11]”, “Ref. [12]" “CIPA[13] was established for exploring the potential of photogrammetry in structural recording”.

There several advantages of close-range photogrammetry which include fast data capture, high level of detail and consistency.“Ref. [14]”, (“Ref [12]”, “Ref. [5]” Other significant advantages stated by “Ref.[15]”are the possibility to extract 3D data and record geometric and textural data simultaneously. The acquired images are usually not the end product but a medium to collect and store the required data which are further processed to derived geometric positions of points or features (objects). The products derived from images are: rectified photos and orthophotos, digital surface models or digital terrain models (DTM), 2D models, 3D models and 2D as well as 3D line drawings. “Ref. [7]”, “Ref. [16]”, “Ref. [9]”

2.4.3 DIFFERENTIAL GLOBAL POSITIONING SYSTEMS

The benefit of integrating GPS and INS, rather than using them standalone, is that they are complementary to each other, which allows more reliable positioning.“Ref. [17]” The integration of GPS and INS was initially carried out for direct georeferencing of airborne laser scanner data. GPS/INS systems were later also used in aerial photogrammetry, either for direct exterior orientation determination or integrated in a bundle adjustment.

The INS consists of an IMU containing accelerometers and gyroscopes and software for data processing. “Ref. [18]” It measures angular and linear movement and can be used for navigation on its own, but due to accumulating errors of the sensors, position data are only reliable for short time periods. An integrated GPS can solve this problem by providing low frequency reference positions to the INS but over longer periods. In return the INS provides high frequency navigation information, valuable if the GPS temporarily loses satellite signal or the number of available satellites falls below the required four. “Ref.[17]” Integrating GPS and INS data is usually performed using a Kalman filter, which requires the physical offset between

the GPS and INS sensors to be considered as (Mirzaei & Roumeliotis [19]). Furthermore, accurate direct georeferencing is only possible if the offsets between GPS/INS and camera can be accounted for and the time is correctly aligned. "Ref. [17]". These offsets can be derived in a calibration procedure that compares exterior orientation parameters derived indirectly based on control points with the results from the GPS/INS measurement "Ref. [20]

GPS/INS is particularly suited for dynamic applications or in areas where the GPS signal is lost easily and therefore sufficient for mapping projects."Ref. [21]"

2.4.4 COMPARISON OF METHODS

Most of literature provides a diverse range of opinions about which method is best suited for mapping. The focus often is on laser scanning and photogrammetry. These techniques can capture a high amount of data in short time and are considered to meet the requirements for urban mapping."Ref. [16]","Ref. [8]","Ref. [12]" A noticeable number of these authors "Ref. [16]","Ref.[23]","Ref. [4]", "Ref. [22]","Ref. [5]" compared different methods of acquiring data and stated that the method to be used should depend on the type of object and the purpose of acquiring. So, no general recommendations can be made and often a combination of different methods is suggested. "Day [24]"remarks that the question is how laser scanning and photogrammetry can complement each other and not which one is the better recording method. This might be probably the reason why various combinations of photogrammetry and laser scanning have been used for urban mapping in recent years.

Previously mentioned mapping methods usually have to be accomplished by people trained in the respective method."Reference [4]","Reference [2]" The skill levels required for interpreting the data differs between mapping methods. For non-specialists it is easier to extract information from a photographic image rather than from a laser scanner point cloud. "Ref. [22]". A further distinctive constraint associated with different mapping methods is cost.

Manual methods are labour intensive as in "Ref. [4]" and laser scanning requires expensive and specialised hardware and software stated in "Ref. [15]". "Böhler and Marbs [15] state that cameras ranging from low-cost to high-end products can be used for photogrammetry". However, to meet the required accuracy level, a camera must meet certain standards, such as providing stable interior orientation, small lens distortions, and sufficient resolution.

3 METHODS AND MATERIALS

3.1 PHOTOGRAPHIC COVERAGE/IMAGE-ACQUISITION.

This is the stage where the images covering the site are acquired by aerial photography. UAS is used to carry out the coverage according to the designed flight plan with 80% overlap (forward) and 70% sidelap (lateral).

3.2 ESTABLISHMENT OF GROUND CONTROL POINT (GCP)

In this stage, the ground control survey is carry out in locating the ground positions of points which can be identified on aerial photographs was established using Trimble Differential Global Position system (DGPS) since is essential for establishing the position and orientation of each photograph in space relative to the ground. This project uses post-marking method since there is no enough controls on these digital images and the photo control points are selected after the aerial image or photography as be acquired.

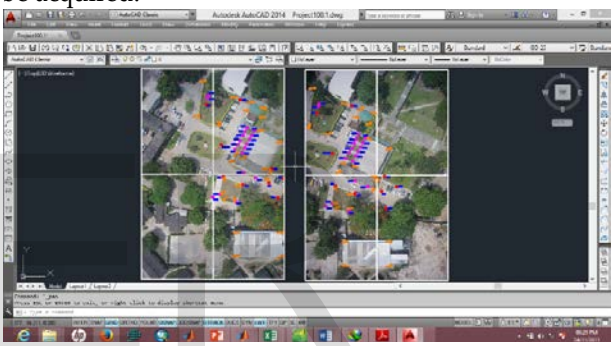

Figure3.2(a) Image strip of overlap area

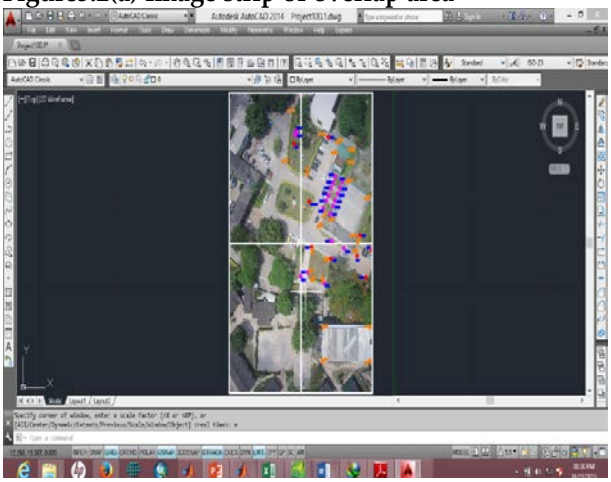

Figure 3.2(b) Control, Check and detail points

3.2.1 FIELD OBSERVATION

This consists of two segments, which are:

- Instrument setting
- Observation

Observations were made after instrument setting and the static mode setting were actualised. Both horizontal and vertical coordinates of the controls and check points on the

stereo image were established on ground at every 30 minutes.

Figure 3.4: Base station on PG 13/17

Figure 3.5: Rovers coordinating a Check Point

Figure 3.6: Tracking of time for the Check points

3.2.2 DATA PROCESSING

This involves the extraction of the data acquired on site from the PROMARK 3 DGPS memory card and GNSS Solutions was used to process the data into their respective x, y and z coordinates with the z-coordinates in orthometric height. The results of the process above are given in the table 4.1.

3.3 MONOCOMPARATOR SIMULATION

In this work, AutoCAD software was used to measure the image coordinates of the point of interests (IOPs) for several times and average obtained. In order to obtain the image coordinates, the coordinates of the four corners of the image were used to establish a mean corrected set of values centered on the geometric center of the image plane. The fig.3.8 illustrates how the image coordinates were obtained. The values of x_o and y_o obtained are taken from every measurement made on the image. The table 3.3 below is image coordinates obtained for this project.

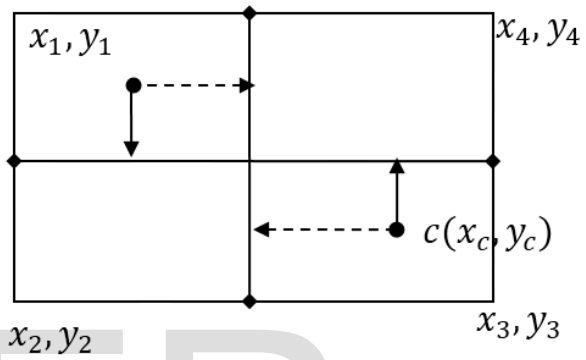

The fig.3.8 illustrates how the image coordinates were obtained

$$x_o = \frac{x_1+x_2+x_3+x_4}{4} \quad (3.1)$$

$$y_o = \frac{y_1+y_2+y_3+y_4}{4} \quad (3.2)$$

3.4 MATHEMATICAL MODELS

These areequationsused in solving a problem at handand the following explain the steps in achieving the geometric positionof GCPs from an acquired drone stereo images.

3.4.1 DEPENDENT PAIR RELATIVE ORIENTATION

The mathematical models"(1)" to "16" is very useful in obtaining relative orientation of stereo pair.

$$b \cdot T_1 \mathbf{x} T_2 = 0 \quad (1)$$

$$P_a = \begin{bmatrix} x_a \\ y_a \\ -c \end{bmatrix}, \quad P_a' = \begin{bmatrix} x_a' \\ y_a' \\ -c \end{bmatrix}, \quad b = \begin{bmatrix} bx \\ by \\ bz \end{bmatrix} \quad (2)$$

$T_1 = [i \,.\, P_a, j \,.\, P_a, k \,.\, P_a]$ (3)

$T_2 = [R_1 \,.\, P_a', R_2 \,.\, P_a', R_3 \,.\, P_a']$ (4)

$b_y = j$, $b_z = k$, $T_{1x} = I$, $T_{1y} = j$ (5)

$T_{2x} = [R_1 \,.\, i, 0, 0]$ (6)

$T_{2y} = [0, R_1 \,.\, j, 0]$ (7)

$T_{2\omega} = [R_{1\omega} \,.\, P_a', R_{2\omega} \,.\, P_a', R_{3\omega} \,.\, P_a']$ (8)

$T_{2\phi} = [R_{1\phi} \,.\, P_a', R_{2\phi} \,.\, P_a', R_{3\phi} \,.\, P_a']$ (9)

T_{2k} = [R_{1k} . $P_{a'}$, R_{2k} . $P_{a'}$, R_{3k} . $P_{a'}$] (10)

$$B = \left[b \cdot T_{1x} \ \mathbf{x} \ T_2 \quad b \cdot T_{1y} \ \mathbf{x} \ T_2 \quad b \cdot T_1 \ \mathbf{x} \ T_{2x} \quad b \cdot T_1 \ \mathbf{x} \ T_{2y}\right] \quad (11)$$

It is used to compute the transform factor:

$$w = (BB^T)^{-1} \quad (12)$$

For matrix A: the elements with respect to the base components (by, bz) are

$$A_1 = w\left[b_y \cdot T_1 \ \mathbf{x} \ T_2 \quad b_z \cdot T_1 \ \mathbf{x} \ T_2\right] \quad (13)$$

and those with respect to the rotation elements (ω, ϕ, k) are

$$A_2 = w\left[b \cdot T_1 \ \mathbf{x} \ T_{2\omega} \quad b \cdot T_1 \ \mathbf{x} \ T_{2\phi} \quad b \cdot T_1 \ \mathbf{x} \ T_{2k}\right] \quad (14)$$

while the constant vector f is obtained as

$$f = -w \ b \cdot T_1 \ \mathbf{x} \ T_2 \quad (15)$$

The contribution for this point to the normal equation is:

$$A_i = \left[A_1 \quad A_2\right], \quad f_1 = f \quad (16)$$

3.4.2 INDEPENDENT PAIR 2D/3D SPATIAL INTERSECTION

The computational modelsused to obtain the ground coordinates by space intersection method are the four collinearity condition equations given as "(17")to "(30)"

$$(k_x c_3 - c_1) \cdot p_A - (k_x c_3 - c_1) \cdot p_o = 0 \quad (17)$$

$$(k_y c_3 - c_2) \cdot p_A - (k_y c_3 - c_2) \cdot p_o = 0 \quad (18)$$

$$(k_x c_3 - c_1) \cdot p_A - (k_x c_3 - c_1) \cdot p_o = 0 \quad (19)$$

$$(k_y c_3 - c_2) \cdot p_A - (k_y c_3 - c_2) \cdot p_o = 0 \quad (20)$$

$$\boldsymbol{c}_1 = \begin{pmatrix} \cos\phi \cos\kappa \\ -\cos\phi \sin\kappa \\ \sin\phi \end{pmatrix} \quad (21)$$

$$\boldsymbol{c}_2 = \begin{pmatrix} \sin\omega \sin\phi \cos\kappa + \cos\omega \sin\kappa \\ -\sin\omega \sin\phi \sin\kappa + \cos\omega \cos\kappa \\ -\sin\omega \cos\phi \end{pmatrix} \quad (22)$$

$$\boldsymbol{c}_3 = \begin{pmatrix} -\cos\omega \sin\phi \cos\kappa + \sin\omega \sin\kappa \\ \cos\omega \sin\phi \sin\kappa + \sin\omega \cos\kappa \\ \cos\omega \cos\phi \end{pmatrix} \quad (23)$$

$$k_x = \frac{x_a}{c}, \ k_y = \frac{y_a}{c}$$

$$k_x' = \frac{x_a}{c}, \ k_y' = \frac{y_a}{c} \quad (24)$$

$$\frac{\partial P_m}{\partial x_m} = i, \ \frac{\partial P_m}{\partial y_m} = j, \frac{\partial P_m}{\partial z_m} = k$$

$$i \cdot j = i \cdot k = j \cdot k = 0 \quad (25)$$

$$A_1 = \frac{c}{k \cdot P_m} \begin{bmatrix} i \cdot i & 0 & k_x k \cdot k \\ 0 & j \cdot j & k_y k \cdot k \end{bmatrix} \quad (26)$$

$$f_1 = -\frac{c}{k \cdot P_m} \begin{bmatrix} k_x k \cdot P_m + i \cdot P_m \\ k_y k \cdot P_m + j \cdot P_m \end{bmatrix}$$

$$H_x' = k_x' C_3 + C_1, \quad H_y' = k_y' C_3 + C_2$$

$$A_2 = \frac{c}{C_3 \cdot \Delta} \begin{bmatrix} H_x' \cdot i & H_x' \cdot j & H_x' \cdot k \\ H_y' \cdot i & H_y' \cdot j & H_y' \cdot k \end{bmatrix} \quad (27)$$

$$f_2 = -\frac{c}{C_3 \cdot \Delta} \begin{bmatrix} H_x' \cdot P_m - H_x' \cdot b \\ H_y' \cdot P_m - H_y' \cdot b \end{bmatrix} \quad (28)$$

Therefore, the two rays yield the design or kernel below.

$$A = \begin{bmatrix} A_1 \\ A_2 \end{bmatrix}, \quad f = \begin{bmatrix} f_1 \\ f_2 \end{bmatrix} \quad (29)$$

$$P_m = P_m + (A^T A)^{-1} A^T f \quad (30)$$

4 RESULTS AND ANALYSIS

4.1 RESULTS

The following were the output of exercisecarried out to achieve the aim and objective of this project:

i. The DGPS coordinates of both control and check points and it corresponding coordinates obtained through bundle adjustment "Table 1."
ii. The difference between the DGPS object coordinates of both control and check points; and the computed object coordinates obtained through bundle adjustment "Table 2."

Table 1

Independent GCPs coordinates obtained by DGPS			Model GCPs coordinates obtained Spatial intersection by Cartesian rays (line equations)		
542595.566	720363.461	6.242	542595.397	720363.420	6.235
542622.636	720383.420	6.497	542622.278	720383.203	6.030
542572.935	720355.142	5.929	542572.742	720355.088	6.169
542571.208	720339.823	5.900	542571.021	720339.819	6.082
542632.938	720359.523	5.240	542633.673	720359.513	5.655
542577.324	720321.538	6.219	542577.927	720321.620	5.953
542589.016	720322.327	6.004	542588.837	720322.398	6.097
542584.176	720311.746	5.916	542583.923	720311.920	5.726
542627.117	720383.488	6.161	542627.515	720383.776	5.601
542629.247	720383.448	6.152	542629.520	720383.662	5.616
542595.360	720352.850	6.115	542594.777	720352.806	6.713
542603.133	720350.768	6.035	542602.709	720350.669	6.440
542607.186	720349.996	6.034	542606.747	720349.870	6.588
542614.312	720348.828	6.003	542613.933	720348.659	6.494
542613.211	720343.068	6.001	542612.634	720343.039	6.892
542609.544	720343.936	5.995	542609.003	720343.866	6.731
542605.920	720344.629	5.983	542605.422	720344.590	6.757
542601.905	720345.335	5.992	542601.502	720345.425	6.658
542558.930	720353.855	5.772	542559.356	720353.874	5.825

542557.077	720340.943	5.737	542557.493	720341.101	5.702
542579.204	720331.814	6.009	542578.780	720332.221	6.438

Table 2

Spatial intersection by Cartesian rays (line equations)		
dx	**dy**	**dz**
0.169	0.041	0.007
0.358	0.217	0.467
0.193	0.054	-0.240
0.187	0.004	-0.182
-0.735	0.010	-0.415
-0.603	-0.082	0.266
0.179	-0.071	-0.093
0.253	-0.174	0.190
-0.398	-0.288	0.560
-0.273	-0.214	0.536
0.583	0.044	-0.598
0.424	0.099	-0.405
0.439	0.126	-0.554
0.379	0.169	-0.491
0.577	0.029	-0.891
0.541	0.070	-0.736
0.498	0.039	-0.774
0.403	-0.090	-0.666
-0.426	-0.019	-0.053
-0.416	-0.158	0.035
0.424	-0.407	-0.429

The root mean square of the residuals from the bundle adjustment of aerial triangulation are shown in appendix A

4.2 ANALYSIS OF RESULTS

4.2.1 ANALYSIS OF GEOMETRIC POSITIONS

The results obtained from the adjustment gave a root mean square error obtained in X, Y and Z for control points to be ±0.392m , ±0.108m , ± 0.273m and it planimetric accuracy is 0.407m (40.7cm); for both control and check points in X, Y and Z is ±0.430m, ±0.152m,± 0.480m and it planimetric accuracy is 0.456m (45.6cm) and for only check points in X, Y and Z is ±0.337m, ±0.232m,±0.164m and it planimetric accuracy is 0.409m (40.9cm). When planimetric or positional accuracy obtained from photo model is compare to that one obtained using DGPS, it reveals that positional accuracy of GCPs from the photo model (0.407m or 40.7cm) is less than that of the DGPS (0.441m or 44.1cm) and result obtained by Musialski et al (2012) who conducted tests on two different sites and achieved a 3D RMSE of 10.5 cm and 42.6 cm, respectively, using a high-end GPS/INS system to provide reference data also agrees with result (positional accuracy = 40.7cm and 40.9cm) obtained for this project. Hence, this provide more confident of a valid solution and the results of the root mean square errors of the measurement's residuals is given in "Table 3", confirm that the obtained precision values from bundle adjustment yielded to acceptable values. Considering the vertical precision of 3D point intersection, which is computed by the average value of photogrammetric base, focal length and error measures in homologous points, and the RMSE of Z coordinate is for the GCPs derived from the image model (0.273) a bit higher than that obtained using DGPS (0.254m) as shown in "Table.3" and "Table.4"

The difference between Independent GCPs obtained from DGPS and drone stereo model for both control and check with their statistics were plotted as shown in Fig."1a", Fig."1b" and Fig."1c" for dx, dy and dz respectively.
These results reveal images with high vertical displacement above tolerable values might be caused by the platform instability, due to atmospheric variations at the time of flight. Similar results were obtained in Gülch, (2012). In his study of the use of fixed wing UAV in photogrammetric procedures, concluded that the external flight conditions do influence images overlaps.

"Table.5" shows distances and difference between these distances for independent GCPs obtained with DGPS and thatobtained from drone image using least square adjustment technique. Also, the relative error and percentage relative error was calculated for lines or distances between GCPs as 0.00265722282 and 0.265722282% respectively as in Table"6". This result gave relative accuracy of 1: 376.3327606 which signify 99.73% as shown in Fig."2". In addition, fig."3" and fig."4" show area selected in the project site and the area of the first and second triangles were calculated. Table "6" gave the results for both areas, their relative error, percentage relative error and relative accuracy. These results as calculated below show that error in the job is minimal since relative accuracy obtained for both first and second triangle are 1:87.66289782 which signify 98.86% and 1:14.8820237 which signify 93.28% respectively.
The distances and heights obtained between GCPs using DGPS and that from the Drone images are given in Fig."7" and Fig."8" respectively.

$$\text{Relative error} = \frac{|\sum(\text{Distance of independent GCPs} - \text{Distance of model GCPs})|}{\text{Distance of independent GCPs}}$$

$$\text{Relative error} = \frac{546.3404374 - 544.8886892}{546.3404374}$$

$$\text{Relative error} = \frac{1.451748279}{546.3404374} = 0.002657223$$

$$\text{Percentage Relative error \%} = 0.002657223 * 100 = 0.265722282\%$$

$$\text{Relative Accuracy} = \frac{1}{0.002657223} = 1:376.3327606$$

Table."3"

Control points coordinates residuals (m) Digital image		
MeanDX= 0.154	MeanDY= 0.012	MeanDZ= 0.075
Rmsex= 0.392	Rmsey= 0.108	Rmsez= 0.273
Control and Check points residuals (m)		
MeanDX= 0.185	MeanDY= 0.023	MeanDZ= 0.230
RmseDX= 0.430	RmseDY= 0.152	RmseDZ= 0.480
Only Check points residuals (m)		
MeanDX= 0.114	MeanDY= 0.054	MeanDZ= 0.027
RmseDX= 0.337	RmseDY= 0.232	RmseDZ= 0.164

Table."4"

Positional accuracy (m)	**Height accuracy (m)**	**Positional accuracy (m)**	**Height accuracy(m)**	**Remark**
GCPs residuals obtained from Drone stereo images (m)		**GCPs residuals obtained from DGPS residuals**		
Only Control residuals (m)				
0.407	0.273	0.441	0.254	Accepted
Control and Check points residuals (m)				
0.456	0.480	0.616	0.523	Accepted
Only Check points residuals (m)				
0.409	0.164	0.487	0.260	Accepted

Table."5"

Point Name	DISTANCE DGPS	DISTANCE DRONE IMAGE	DIFFERENCE
13/17			
3	33.63252267	33.37596815	0.25655452
4	57.18246834	56.95848068	0.22398766
5	15.41604002	15.36568261	0.05035742
6	64.79724454	65.67439943	-0.8771549
7	67.34817905	67.40545946	-0.0572804
8	11.71859143	10.9377047	0.78088673
9	11.63542698	11.57306701	0.06235997
11	83.61126745	84.0449118	-0.4336444
12	2.130375554	2.008238283	0.12213727
13	45.65705173	46.46685684	-0.8098051
15	8.047002734	8.214827631	-0.1678249
16	4.125868757	4.116290199	0.00957856
18	7.221087176	7.287325778	-0.0662386
19	5.864281797	5.768171374	0.09611042
20	3.768330267	3.723988453	0.04434181
21	3.689664619	3.653455488	0.03620913
22	4.076599195	4.007945234	0.06865396
26	43.81142574	42.98454277	0.82688297
27	13.0442843	12.90814851	0.13613579
29	23.93622297	23.06492508	0.87129789
13/17	35.62650212	35.34829968	0.27820244
Distance Sum	546.3404374	544.888689	

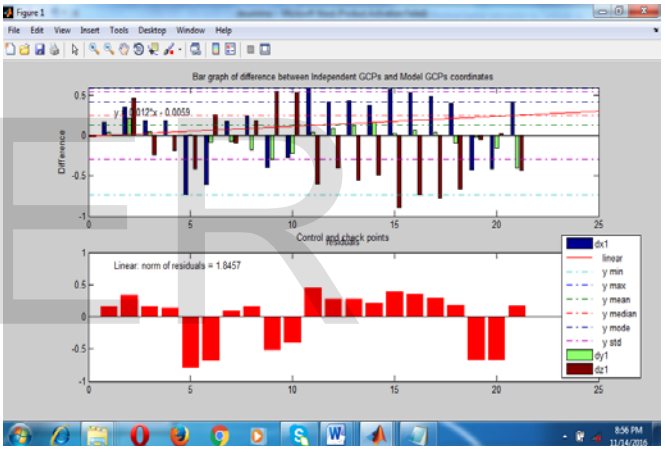

Fig."1(a)"

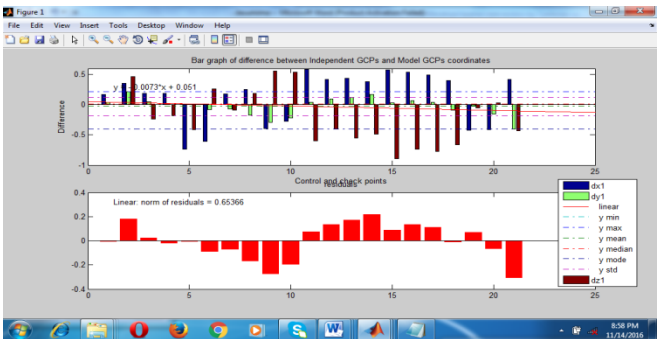

Fig."1(b)"

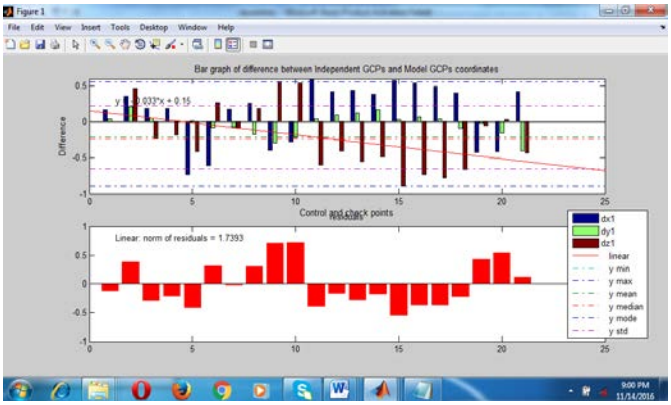

Fig."1(a)"

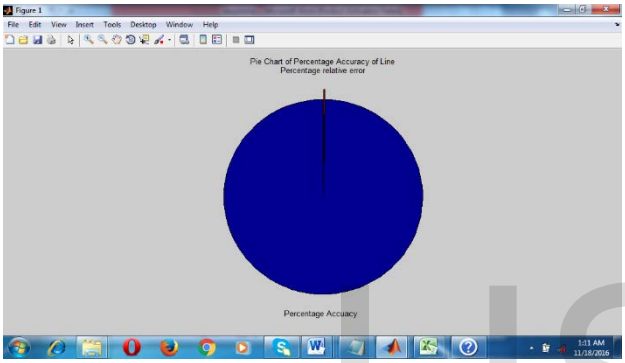

Fig. "2"

FIRST TRIANGLE

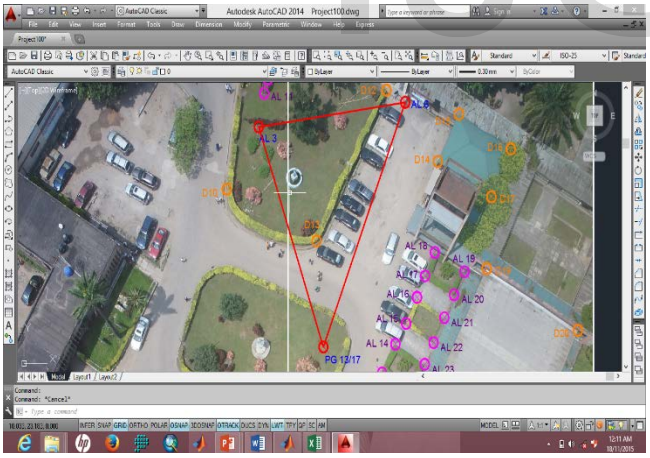

Fig "3"

Relative error

$$= \frac{|\,(\text{Area of independent GCPs} - \text{Area of model GCPs})\,|}{\text{Area of independent GCPs}}$$

$$\text{Relative error} = \frac{|\,(426.254704 - 431.119087)\,|}{426.254704} = 0.011411916$$

$$\text{Percentage Relative error \%} = 0.011411916 * 100 = 1.141191629\%$$

$$\text{Relative Accuracy} = \frac{1}{0.01140733} = 1:87.66289782$$

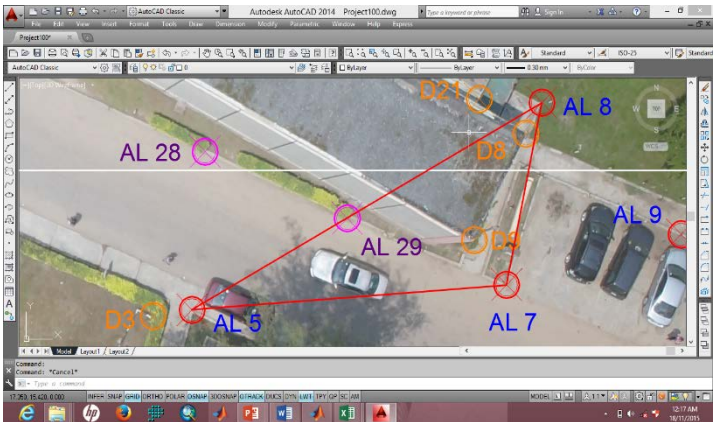

Fig."4"

Relative error

$$= \frac{|\,(\text{Area of independent GCPs} - \text{Area of model GCPs})\,|}{\text{Area of independent GCPs}}$$

$$\text{Relative error} = \frac{|\,(109.306872 - 101.961979)\,|}{109.306872} = 0.06719516$$

$$\text{Relative error \%} = 0.06719516 * 100 = 6.719516$$

$$\text{Relative Accuracy} = \frac{1}{0.06719516} = 14.882023$$

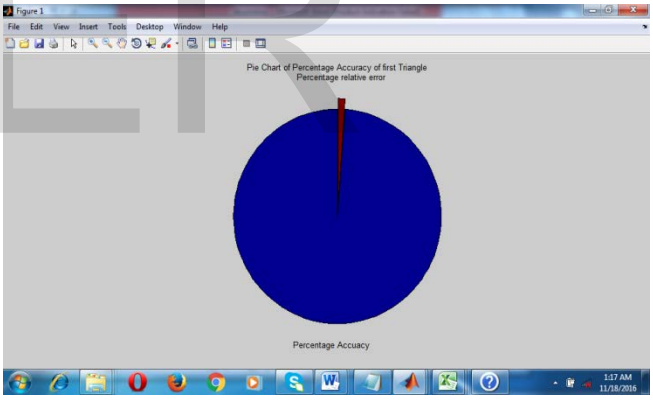

Fig."5"

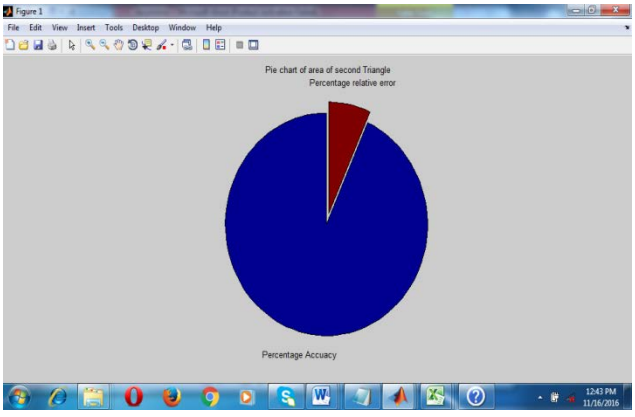

Fig."6"

Table. "6"

Shape	Indep GCPs	Model GCPs	Rel. error	Per. Rel. error (%)	Rel. Accuracy	Per. Accuacy (%)
Line	1.356652798		0.003	0.25	1:402.72	99.73
Area of first triangle	426.25	431.12	0.011	1.14	1:87.66	98.86
Area of second triangle	109.31	101.96	0.067	6.72	1:14.88	93.28

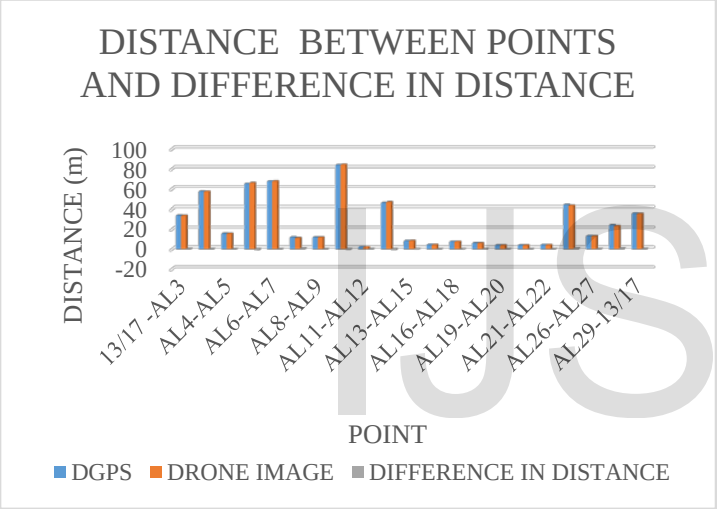

Fig."7"

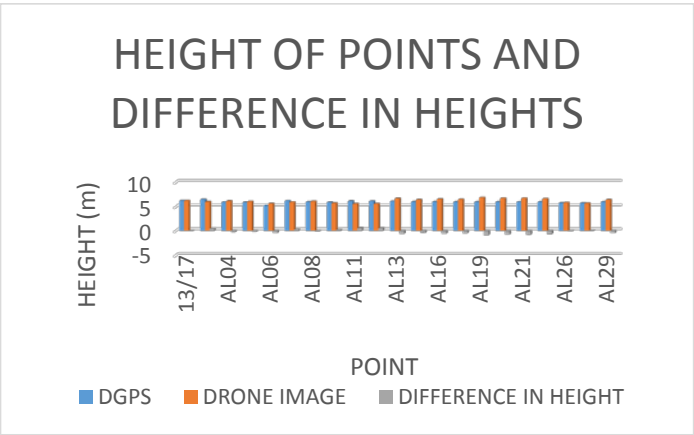

Fig."8"

4.2.2 STATISTICAL ANALYSIS

"Table 7"and Fig."9"shows the results obtained for The ANOVA *F*-test thatwas used to assess whether distances obtain between GCPs using DGPS is on average superior, or inferior, to the distances obtain between GCPs using acquired drone images versus the null hypothesis that the two distances groups yield the same mean distances. The critical value from the statistical table is given as $F_{crit}(1,48) = 4.08$ at $\alpha = 0.05$ and when this value is compare with F calculated ($7.88396e^{-05}$) using matlab, the F calculated is smaller or less than F_{crit} (i.e $F=7.88396e^{-05} < 4.08$). This implies that the result is insignificant (same) at the 5% significance level and that the null Hypothesis will be accepted; and therefore there is strong evidence that the expected values in the two groups highly insignificance (same). The probability value (p-value) for this test is 0.993 as in table "7" which is greater than 0.05 and this shows that the result (planmetric positions) is insignificant (same) at the 5% significance level and that the null Hypothesis will be accepted. So, there is high confident that the mean distance between GCPs usingDGPS are the same with the mean distance obtained from drone images.

Also, "Table 8" shows the results obtained for The ANOVA *F*-test was used to assess whether heights obtain between GCPs using DGPS is on average superior, or inferior, to the distances obtain between GCPs using acquired drone images versus the null hypothesis that the two distances groups yield the same mean distances. The critical value from the statistical table is given as $F_{crit}(1,48) = 4.08$ at $\alpha = 0.05$ and when this value is compare with F calculated (3.99) using matlab, the F calculated is lower or less than F_{crit} (i.e $F=3.99 < 4.08$). This implies that the result is insignificant (same) at the 5% significance level and that the null Hypothesis will be accepted; and therefore there is low evidence that the expected values in the two groups are the same. The probability value (p-value) for this test is 0.0526 as in Table "8" which is greater than 0.05 and this also shows that the result is insignificant (same) at the 5% significance level and that the null Hypothesis will be accepted. So, there is low confident that the heights mean between GCPs using DGPS are the same with the heights mean obtained from drone images.

Table "7"

ANOVA TABLE FOR DISTANCES					
Source	SS	df	MS	F	Prob > F
Columns	0.1	1	0.05	$7.88396e^{-05}$	0.993
Error	25459.4	40	636.486		
Total	25459.5	41			

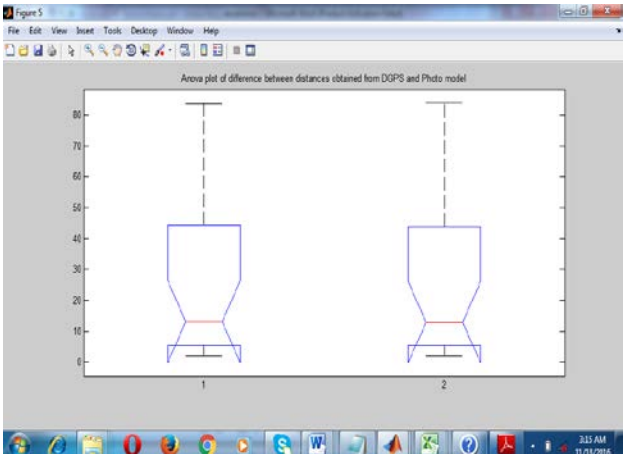

Fig."9"

Table "8"

ANOVA TABLE FOR HEIGHTS					
Source	SS	df	MS	F	Prob > F
Columns	0.47488	1	0.47488	3.99	0.0526
Error	4.75941	40	0.11899		
Total	5.23429	41			

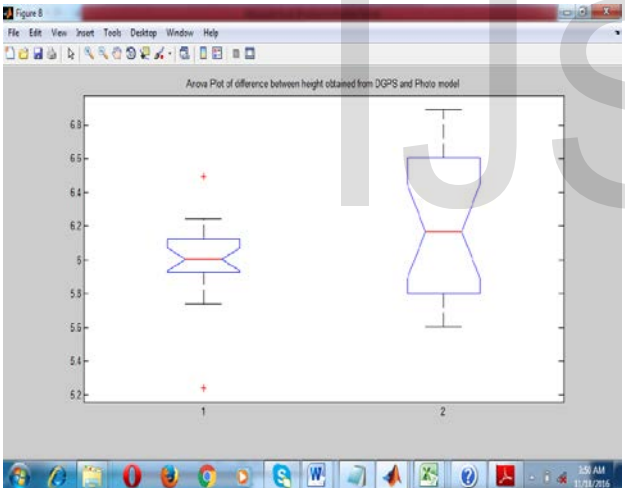

Fig."9"

5 CONCLUSIONS AND RECOMMENDATION

5.1 CONCLUSIONS

The data acquired from this technology in University of Lagos proved even more that UASs offer a far-reaching new approach to mapping and spatial data acquisition process in that there is high agreement between geometric coordinates of GCPs obtained with DGPS and that obtained with drone image. The test of analysis of variance shows that the distance mean obtained with both techniques is the same or highly insignificant. These results reveal images with high vertical displacement above tolerable values whichmight be caused by the platform instability, due to atmospheric variations at the time of flight or might be due to inability to read image coordinates to higher accuracy. Similar results were obtainedin [15]. In his study of the use of fixed wing UAV in photogrammetric procedures, concluded that the external flight conditions do influence images overlaps.

This new approach would enable individuals or small firms in developing countries to acquire mapping capacities which could deliver current spatial data at unprecedented resolutions. It also promises to save time and cost over earlier conventional mapping techniques or approaches.

This paper shows and discusses the obtained results from the conducted study area carry out in the Faculty of Education, University of Lagos, Akoka Yaba, Lagos state. The photogrammetric flight was performed with a flight height nearly to 100 m by using Trimble UAS drone (UX-5), digital images were automatically taken. The images have a Ground Spatial Resolution 2.4cm to 24cm. By considering the obtained results from the work phases, the main conclusions can be drawn:

i. Using a UAV system, the geometric characteristics of photogrammetric flight can vary significantly from what it was planned. The platform instability due to atmospheric variations at the moment of the flight can cause significant variation in the area covered by the image, forward and sidelap overlaps;

ii. The monocomparator used to measured image coordinates might not give best values for each position of interest. So, automatic reading of image coordinates will have produced the best estimates of geometric positions (x, y and z).

iii. From the analysis of checkpoints discrepancies, the performed bundle adjustment achieved horizontal accuracy close to 0.407m. This accuracy is higher than that ofDGPS (expected value) of 0.441m on the ground while the vertical accuracy obtained from drone image (0.273) is higher than that of DGPS (0.254) The most likely cause for this inaccuracy is the deficiency of control points on the block`s border, caused by the impossibility to find recognizable photogrammetric details in this cluster environment;

5.2 RECOMMENDATION

The following recommendations are suggested for further photogrammetry works:

- I recommend that any future research in the field of digital photogrammetric works should use an image matching technique for increasing the accuracy of measuring image coordinates.
- I recommend Future research work should focus on developing methods to increase the accuracy of

the direct determination of the image`s exterior orientation parameters and use them in the aerial triangulation procedure in order to decrease the number of used control points on the block.

- I recommend that this new approach would enable individuals or small firms in developing countries to acquire mapping capacities which could deliver current spatial data at unprecedented resolutions and it can also save time and cost over earlier conventional mapping techniques or approaches.

ACKNOWLEDGMENT

The authors wish to thank Mr Babajide Yusuf and non-academic staff of University of Lagos for the assistant rendered during the field work.

AUTHORS

1 Prof. Olaleye J.B
Department of Surveying and Geoinformatics
University of Lagos, Akoka, Lagos.

2 Suru W.P.
Department of surveying and Geoinformatics
Federal Polytechnic Ede, Osun State.

3 Odeyemi F.G.
Department of surveying and Geoinformatics
Federal Polytechnic Ede, Osun State.

4 Alabi A.O.
Lagos state Ministry of Surveying
Alausa IKeja, Lagos

REFERENCES

[1] W.Volkmann and G. Barnes Virtual Surveying: Mapping and Modelling Cadastral. *FIG Congress*, 2.

[2] C.Achille,C.Monti,C. C. Monti and C.Savi "Survey and representation of the Villa Reale di Monza to support of the International Design Competition.*"CIPA XX International Symposium 2005,*Torino, Italy.

[3] C.Campanella,M. Tessoni,S.Bortolotto, E.Ciocchini and F.Zangheri. "Basilica of Saint Peter Martyr from Verona in S. Anastasia (Verona): Structures geometric survey and photographic campaign for the preservation project.*"CIPA XX International Symposium 2005*, Torino, Italy.

[4] N. Haddad andT. Akasheh "Documentation of archaeological sites and monuments: Ancient theatres in Jerash*".CIPA XX International Symposium 2005,*Torino, Italy.

[5] P. Grussenmeyer, T. Landes, T. Voegtle andK. Ringle "Comparison methods of terrestrial laser scanning, photogrammetry and tacheometry data for recording of cultural heritage buildings."*International Archives of Photogrammetry, Remote Sensing International Archives of Photogrammetry, Remote Sensing and Spatial Information Sciences* 2008, pp. 37(B5),pp. 213-218.

[6] EnglishHeritage. "Metric Survey Specifications for English Heritage."*Swindon., 2008*. (p. 111 pages).

[7] Clowes, M. "Digital photogrammetry at English Heritage" a pictorial review of projects to date. *Photogrammetric Record*2002, 17(99), pp. 441-452.

[8] V.A. Girelli, M.A. Tini, andA. Zanutta "Traditional and unconventional photogrammetric techniques for metrical documentation of cultural heritage: The example of the—Rolandino Dei Passaggieri‖ Tomb (St. Domenico Square) survey in Bologna." CIPA XX International Symposium 2005, Torino, Italy.

[9] F. Tack, J. Debie, R. Goossens, J. De MeulemeesterandD. Devriendt "A feasible methodology for the use of close range photogrammetry for the recording of archaeological excavations*".CIPA XX International Symposium 2005*, Torino, Italy.

[10] H.M. Yilmaz, M. Yakar, S.A. Gulec and O.N. Dulgerler"Importance of digital close- range photogrammetry in documentation of cultural heritage". *Journal of Cultural Heritage*2007, 8(4),pp. 428-433.

[11] J.H. Chandler, P. Bryan andJ.G. Fryer " The development and application of a simple methodology for recording rock art using consumer-grade digital cameras."*Photogrammetric Record*2007, pp. 22(117), pp. 10-21.

[12] E.Ö Avşar, Z. Duran, O. Akyol andG. Toz" Modeling of the Temple of Apollo Smintheus using photogrammetry and virtual reality."*International Archives of the Photogrammetry, Remote Sensing and Spatial Information Sciences*2008, 37(B5), pp. 357-360,.

[13] CIPA. "*CIPA Web Site – Objectives*."2010

[14] B. Blake "*Metric survey techniques for historic buildings. In: Structures & Construction in Historic Building Conservation, (Ed. Forsyth, M.*2007*).* WileyBlackwell, Oxford..

[15] J.G. Fryer, H. Mitchell andJ.H. Chandler "*Applications of 3D measurement from images."* (Dunbeath – Caithness, Ed.) Whittles Publishing, 2007.

[16] W. Böhler andA. Marbs " 3D scanning and photogrammetry for heritage recording: A comparison."*12th International Conference on Geoinformatics 2004*, (pp. pp. 291-298). Gävle, Sweden.

[17] M. Cramer andD. Stallmann " On the use of GPS/inertial exterior orientation parameters in airborne photogrammetry". 2002,

[18] C. Heipke, K. Jacobsen, H. Wegmann, O. Andersen andB. Nilsen " Test Goals and Test Set Up for the OEEPE Test —Integrated Sensor Orientation Ⅱ."*In: OEEPE Integrated Sensor Orientation Test Report and Workshop* (Eds. C. Heipke, K. Jacobsen andH. Wegmann)

[19] F.M. Mirzaei andS.I. Roumeliotis " A Kalman filter-based algorithm for monitored in 3D using miniature accelerometers and earth-magnetic field sensors." 2008'

[20] G. Forlani andL. Pinto "Integrated INS/DGPS systems: calibration and combined block adjustment."*In: OEEPE Integrated Sensor Orientation Test Report and Workshop* 2002, Torino, Italy.

[21] A. El-Rabbany " Introduction to GPS: the global positioning system."*Artech House 2006*, 210 pages.

[22] Ardissone, P., Bornaz, L., Lo Turco, M. And Vitali, M. (2005). The relief of the Porta Palatina: A comparison between different survey methodologies and representations. *CIPA XX International Symposium 2005,*, pp. 86-90.

[23] D.P. Andrews, N.J Beckett, M. Clowes and S.M. Tovey "A comparison of rectified photography and orthophotography as applied to historic floors – with particular reference to Croughton Roman Villa."*CIPA XX International Symposium 2005*, pp. 77-81.

[24] N. Day "Terrestrial photogrammetry as an alternative to laser scanning."*Geomatics World 2010, 18(2)*, pp. 36-38.

[25] Gülch, E., 2012 "Photogrammetric measurements in fixed wing UAV imagery."*ISPRS– Int. Arch. Photogramm. Remote Sens. Spatial Inform. Sci. XXXIX-B1*, 381–386.